



AUTHOR(S):

TITLE:

YEAR:

Publisher citation:

OpenAIR citation:

Publisher copyright statement:

This is the _____ version of an article originally published by _____
in _____
(ISSN _____; eISSN _____).

OpenAIR takedown statement:

Section 6 of the "Repository policy for OpenAIR @ RGU" (available from <http://www.rgu.ac.uk/staff-and-current-students/library/library-policies/repository-policies>) provides guidance on the criteria under which RGU will consider withdrawing material from OpenAIR. If you believe that this item is subject to any of these criteria, or for any other reason should not be held on OpenAIR, then please contact openair-help@rgu.ac.uk with the details of the item and the nature of your complaint.

This publication is distributed under a CC _____ license.

Influence of Pr doping on the structural, morphological, optical, luminescent and nonlinear optical properties of RF sputtered ZnO films

R.Sreeja Sreedharan¹, R.Vinod Kumar^{1,2}, I. Navas¹, Radhakrishna Prabhu³, and V.P. Mahadevan Pillai^{1*}

¹Department of Optoelectronics, University of Kerala, Kariavattom, Thiruvananthapuram, Kerala 695581, India.

²University College, Thiruvananthapuram, Kerala, India.

³School of Engineering, Robert Gordon University, Aberdeen, UK.

*For correspondence email: vpmpillai9@gmail.com

Abstract

The effects of Pr doping on the structural, morphological, optical and non-linear optical properties have been investigated. XRD and Raman analysis reveals the formation of highly c-axis oriented films with hexagonal wurtzite structure of ZnO. AFM and SEM images reveal the formation of grains with well-defined grain boundaries. The Pr doped films presents excellent optical transparency in the visible region. The PL spectra show both UV and visible emissions and the intensity of the visible emission increases with Pr doping. Nonlinear optical properties of the Pr incorporated ZnO nanostructures have been investigated using open aperture Z-scan technique. It is interesting to note that 1wt% Praseodymium incorporated ZnO film shows saturable absorption, whereas the 5wt% Praseodymium incorporated ZnO shows reverse saturable absorption and the high value of non-linear absorption coefficient (β) for 5wt% Pr doped ZnO film suggests the suitability these films for optoelectronic device applications.

Keywords

Pr doped ZnO films, rf magnetron sputtering, micro-Raman spectra, defect emission, Z-scan technique.

1. Introduction

ZnO has attracted much interest as a nonlinear optical (NLO) material with high NLO response, which makes it a potential candidate for NLO based device applications such as optical switching devices, three dimensional fluorescence imaging, and optical limiting [1]. The increased demand of low-voltage electronics have enhanced the need for zinc oxide based varistors with fast response, high non-linear current-voltage characteristics and energy absorption capabilities at low breakdown voltage [2]. Zinc oxide is a versatile material that has achieved applications in photo catalysts, solar cells, [3] chemical sensors [4], piezoelectric transducers, transparent electrodes, electro luminescent devices [5], ultraviolet laser diodes, field effect transistors [6, 7, 8] etc. Rare-earth doped semiconductors have received considerable attention as technologically important material for optoelectronic device applications [9]. Rare-earth metals are chosen as dopants because of their long-lived, spectrally narrow luminescence emissions in the visible range of the spectrum at its trivalent form. The luminescence is caused by their 4f intra-shell transitions which can result in intense line spectra [10]. In addition to this 4f intra-shell transition, rare earth ion may stabilize intrinsic defect sites which could also give rise to broad emission in the visible region [10]. ZnO is a good host for incorporating rare earth elements and easily produces intrinsic defects such as

interstitial zinc and oxygen vacancy. The large exciton binding energy (60 meV at room temperature)[11, 12, 13] and wide direct band gap energy (3.37 eV) of ZnO[14, 15] leads to efficient energy transfer from exciton to rare earth ion [16]. Therefore the optical properties of rare earth doped ZnO nanostructures are expected to be modified remarkably. However, it is difficult to incorporate rare earth ion into semiconductor nanostructures. Even if rare earth ions have been doped in to ZnO lattice, it may be located at grain boundary as activators and hence no luminescence arising from rare earth ion may be observed [17]. Praseodymium added ZnO ceramics is considered to be a potential host material for varistor applications. Praseodymium oxide added in ZnO is observed to be segregated at the grain boundary of ZnO ceramics and helps to form a double Schottky barrier which is thought to be the origin of varistor characteristics [18]. Among the rare-earth materials, the properties of praseodymium doped zinc oxide films have not yet been studied extensively. In this work Pr doped ZnO thin films (with doping concentration 0, 1, 3 & 5 wt%) were prepared by RF magnetron sputtering and their structural, morphological, optical and non-linear optical properties were investigated in detail.

2. Experimental

Radio frequency magnetron sputtering technique is used for the growth of pure and Pr doped ZnO film on quartz substrate. The target is prepared from commercially available ZnO and Pr₂O₃ powders (Aldrich – purity 99.99 %). The pressed powders of pure and Pr₂O₃ incorporated ZnO with doping concentrations 1, 3 & 5 wt% are used for the film fabrication. The chamber is evacuated to a base pressure of 3×10^{-6} mbar and argon flow rate was adjusted in order to keep the desired gas pressure at 4×10^{-2} mbar. The films are deposited for 30 minutes on cleaned quartz substrates kept at a distance 5 cm away from the target. The RF radiation for sputtering the film is adjusted at a power level of 150 watts. The as deposited films thus prepared with Pr doping concentrations 0, 1, 3 & 5 wt% are designated as P0, P1, P3 and P5 respectively.

The structural information of the as deposited films are studied by X-ray diffraction technique using a Bruker AXS D8 Advance X-ray diffractometer equipped with X-ray source KRISTAOFLXE 780, KF.4KE with wavelength $\sim 1.5406 \text{ \AA}$. The micro-Raman spectra of the films are recorded using Labram-HR800 spectrometer using radiation from an argon ion laser with wavelength 488 nm. The spectra are acquired by 1800 grids/nm grating, a super-notch filter with a cut off at 50 cm^{-1} and a Peltier cooled CCD camera having a spectral resolution of about 1 cm^{-1} . The elemental analysis and surface morphology of the films are studied using a Scanning Electron Microscope (JEOL-JSM 5600) equipped with EDAX attachment. The optical transmission spectra of the films are recorded in the wavelength range of 200-900 nm using JASCO V-550 UV-visible double beam spectrophotometer. Photoluminescence spectra of the samples are recorded by Horiba Jobin Yvon Fluorolog III modular spectrofluorometer equipped with 450 W Xenon lamp and Hamatsu R928-28 photomultiplier with a computer attached to the setup. The thicknesses of the films are measured using Daktak 6M stylus profile meter. The nonlinear optical properties of the Pr doped films were studied using open aperture z-scan measurements. A frequency doubled laser radiation at wavelength 532 nm (pulse width 7 ns, repetition frequency 10 Hz) with beam waist radius $14 \text{ }\mu\text{m}$ and peak intensity $8 \times 10^{-8} \text{ J/m}^2$ from a Q-switched Nd: YAG laser is used for the non-linear optical measurements

3. Results and Discussion

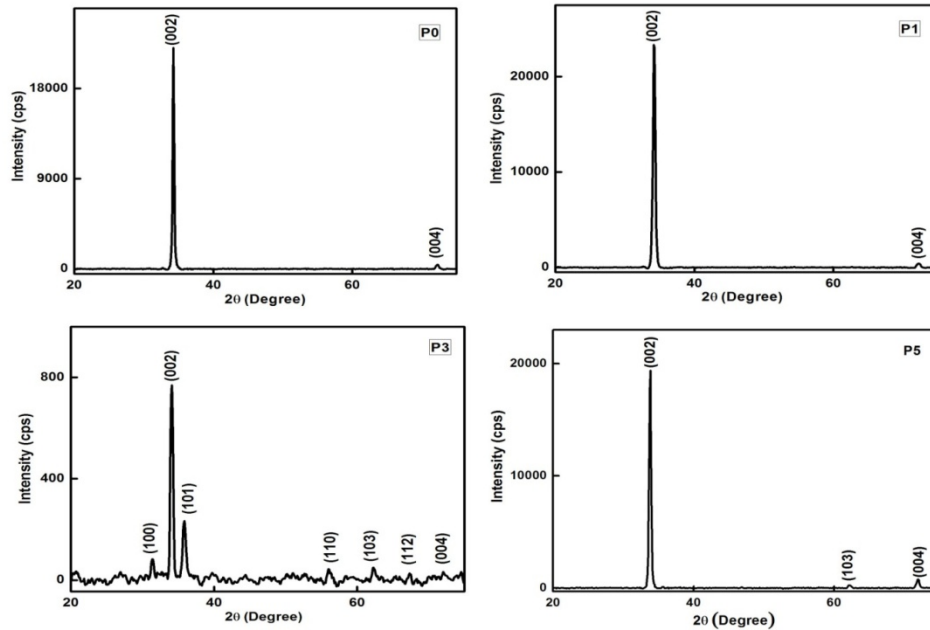


Fig. 1 XRD patterns of undoped and Pr doped ZnO films with doping concentrations 0, 1, 3 and 5 wt%.

The X-ray diffraction patterns of the undoped and PrdopedZnO films are shown in Fig.1. The diffraction peaks in all the films can be indexed to hexagonal wurtzite structure of ZnO. [JCPDS 00-005-0664]. It is seen that all the films show sharp and intense XRD peaks indicating the good crystalline quality of the films. The 1wt% Pr doped ZnO film shows an enhancement in intensity compared to that of theundoped film. The XRD pattern of 3wt% PrdopedZnO film shows a reduction in intensity, but with the appearance of several medium to weak peaks indicating the polycrystalline nature of the film.The 5wt% Prdoped ZnO film also shows an enhancement inintensitycompared to that of the 3wt% Prdoped ZnO film. The X-ray diffraction patterns of all the films present a very intense peak corresponding to the lattice reflection plane (002) indicating that the crystalline growth is along $\langle 001 \rangle$ direction in them. Preferential orientation of the grains along the (002) plane is commonly observed in films with hexagonal wurtzite structure, which can be due to the lowest surface free energy of (002) plane based on thermodynamics [19, 20, 21].Based on epitaxial growth theory of thin films, the epitaxial growth of the thin film is expected to be in accordance with the matching relation of the lattice constant between the thin film and substrate. Since quartz is an amorphous material, there is no lattice matching mechanism between the ZnOfilm and amorphous fused quartz. Hence the growth of the film is mainly determined by the balance of interfacial energy of the film and fused quartz. The interfacial energy is related to atomic plane density in the interface between film and fused quartz [22, 23]. Information regarding the parameters that characterizes the growth such as lattice constants, average crystallite size,defect density, lattice strain, and stress are extracted from the XRD measurements.

In the Pr_2O_3 ; ZnO system there is a possibility that Pr^{3+} ion may occur either as a substituent for Zn^{2+} ion or as segregation in the grain boundary region [24, 25, 26,27, 28]. If Pr^{3+} ionsare substitutedfor Zn^{2+} ions, a

corresponding peak shift would be expected in the diffraction pattern. Since the ionic radius of Pr^{3+} ion (1.13\AA) is higher than that of Zn^{2+} ion (0.74\AA), the substitution of Pr^{3+} ion will result in the expansion of lattice which will increase the lattice parameters and the peak may shift to lower 2θ values [29]. The (002) diffraction peak for undoped ZnO film is observed at 2θ value 34.26° . A continuous shift towards lower values of 2θ is observed for the intense (002) diffraction peak of ZnO with Pr doping. This indicates the possibility of substitution of Pr^{3+} ion in the ZnO lattice. No diffraction peaks from Pr_2O_3 or other impurities are found in any of the samples within the detection limit suggesting the successful replacement of Pr^{3+} ions for Zn^{2+} ions in the ZnO lattice.

In order to get more information about the micro-structure of the films, we calculated the lattice parameter 'c' of hexagonal crystal structure (Table. 1) using the formula

$$\frac{1}{d_{hkl}^2} = \frac{4}{3} \left(\frac{h^2 + hk + k^2}{a^2} \right) + \frac{l^2}{c^2} \quad (1)$$

where a and c are the lattice constants, h, k, l are the miller indices of the planes and d_{hkl} is the inter planar distance. The calculated values of lattice parameter 'c' of the films are given in Table 1. The lattice parameter 'c' obtained for the pure ZnO film is 0.5247 nm and its value increases with increase in Pr doping concentration. This indicates that the unit cells are elongated along the c axis, and compressive forces act along the plane of the films. The increase in the value of c-lattice parameter with Pr doping also supports the substitution of Pr^{3+} ion into Zn^{2+} sites. Alireza Khataee *et al.* and Ilanchezhian *et al.* also reported similar observation in Pr doped ZnO films [27, 28]

Different factors such as difference in thermal expansion coefficients (TEC) of the film and the substrate, lattice mismatch between the film and substrate, ionic size mismatch between the dopant and host cation, presence of impurities and defects in the films, deposition conditions etc., may contribute towards the stress in the films [29]. The presence of defects such as oxygen vacancies can also result in the volume expansion of the lattice introducing strain in the film. Navas *et al.*, suggested that the substitution of a cation with ionic radius different from that of host cation introduces a stress in the lattice and can affect the size of the unit cell [30].

Table. 1 Structural and optical parameters of undoped and Pr doped ZnO films with doping concentrations 0, 1, 3 and 5 wt%.

Film	d_{hkl} (nm)	FWHM	D_{hkl} (nm)	δ (m^{-2})	C (nm)	Strain	Bi-axial Stress (G Pa)	Bandg ap (eV)	Thickness (nm)
P0	0.2623	0.2302	36	7.57×10^{14}	0.5247	0.8015	-3.6356	2.94	77
P1	0.2627	0.3652	23	1.91×10^{15}	0.5254	0.9406	-4.2665	3.02	74
P3	0.2636	0.2285	37	7.85×10^{14}	0.5271	1.2698	-5.7599	3.06	70
P5	0.2657	0.3308	25	1.64×10^{15}	0.5314	2.0917	-9.4881	2.96	78

The lattice stress σ_f of the films are calculated from XRD data using biaxial strain model by comparing the c-lattice constant to the strain-free lattice parameter measured from ZnO powder sample[31]. The strain along the c-axis is calculated using the expression

$$\varepsilon(\%) = \frac{c - c_0}{c_0} \times 100 \quad (2)$$

where ε is the strain in the direction of the c-axis, perpendicular to the substrate surface, c_0 (5.205 Å) is the c-axis lattice constant of bulk ZnO obtained from JCPDS data card and c is the c-axis lattice constant calculated from the XRD peak position. The undoped film shows minimum value of strain and the strain is found to be increasing with Pr doping. Combined with elastic constants of single crystalline ZnO, the stress in the films along c-axis is given by [32]

$$\sigma = -453.6 \frac{c - c_0}{c_0} \times 10^9 \text{ Pa} \quad (3)$$

The negative sign in equation (3) corresponds to compressive stress for lattice expansion. The calculated stress values are given in Table 1. The negative sign of calculated stress for all the films indicates that the crystallites are in a state of compressive stress. Based on earlier investigations, it can be seen that residual stress always exists in ZnO films originating from intrinsic and extrinsic stresses [33, 34, 35]. The intrinsic stress is associated with impurities and defects in the film. The extrinsic stress mainly arises from the lattice mismatch between substrate and ZnO film as well as thermal mismatch induced by difference in TEC of substrate and the film [36]. Ohshima *et al.*, studied the dependence of the ZnO film crystallinity on the substrate material and reported that highly oriented ZnO films can easily be grown on a single crystal substrate rather than other amorphous substrates [37]. Due to the amorphous nature of quartz, it is difficult to calculate the stress induced by lattice mismatch between ZnO film and quartz substrate [38]. Verghese *et al.*, reported that the appreciable anisotropy in thermal expansion of ZnO, due to its uniaxial nature gives rise to residual stress upon cooling from fabrication temperature [39]. The thermal effects due to electron impact on the substrate produces substrate heating during sputtering. The samples are not heated externally, but due to energy flux during sputtering the temperature rises. The maximum temperature observed during sputtering by monitoring the substrate temperature using thermocouple is below 100°C. This yields significantly small thermal stress due to thermal mismatch in comparison with the observed stress in the films. The stress values indicate that the doping strongly influences the stress in the films [40, 41]. Hence it can be inferred that doping is an important factor that causes lattice distortion due to the difference in ionic radii of dopant (Pr^{3+}) and host cations (Zn^{2+}).

The average size of the crystallite in the films can be calculated from the well-known Debye-Scherrer formula[42]. It is found that the average crystallite size in the films varies between 23-37 nm confirming the nanostructured nature of the films (Table. 1). It can also be seen that a moderate doping of ZnO with Pr increases

the crystallinity of the films. The dislocation density (δ) represents the length of the dislocation line per unit volume in the film. The value of dislocation density in the films was calculated (Table. 1) using the following formula;

$$\delta = \frac{1}{D_{hkl}} \quad (4)$$

The lower value of the dislocation density shows the better crystalline quality of the films [43].

Raman spectral analysis has been carried out to obtain more information about the micro-structure of the films. Raman spectroscopy is a non-destructive way of probing the crystal structure, phonon frequencies, composition and defects in semiconductors [44]. The ZnO wurtzite hexagonal crystal structure belongs to space group $P6_3mc(C_{6v}^4)$ in the group theory with two formula units per primitive cell. The factor group analysis of the compound is carried out using the correlation method developed by Fateley *et al.* [45]. Excluding the acoustic modes at the Brillouin zone centre $k=0$, the nine optical modes under the factor group C_{6v} are given by

$$\Gamma_{optical} = A_1 + 2B_1 + E_1 + 2E_2 \quad (5)$$

Out of these, A_1 and E_1 modes are active in both IR and Raman spectra and E_2 mode is active only in Raman spectra. The B_1 modes are inactive both in IR and Raman spectra. However due to the lowering of symmetry, the inactive B_1 mode may become active and the degeneracy of the E_1 and E_2 modes may get lifted. The E_2 modes consist of two modes of low and high frequency phonons. The A_1 and E_1 modes split into transverse (TO) and longitudinal optical (LO) components with different frequencies [46]. Based on the results obtained from earlier investigation, the various Raman modes of the ZnO films can be expected as follows: $E_2(low) \sim 101 cm^{-1}$, $E_2(high) \sim 437 cm^{-1}$, $A_1(TO) \sim 380 cm^{-1}$, $A_1(LO) \sim 574 cm^{-1}$, $E_1(TO) \sim 407 cm^{-1}$, $E_1(LO) \sim 584 cm^{-1}$ [36, 47, 48].

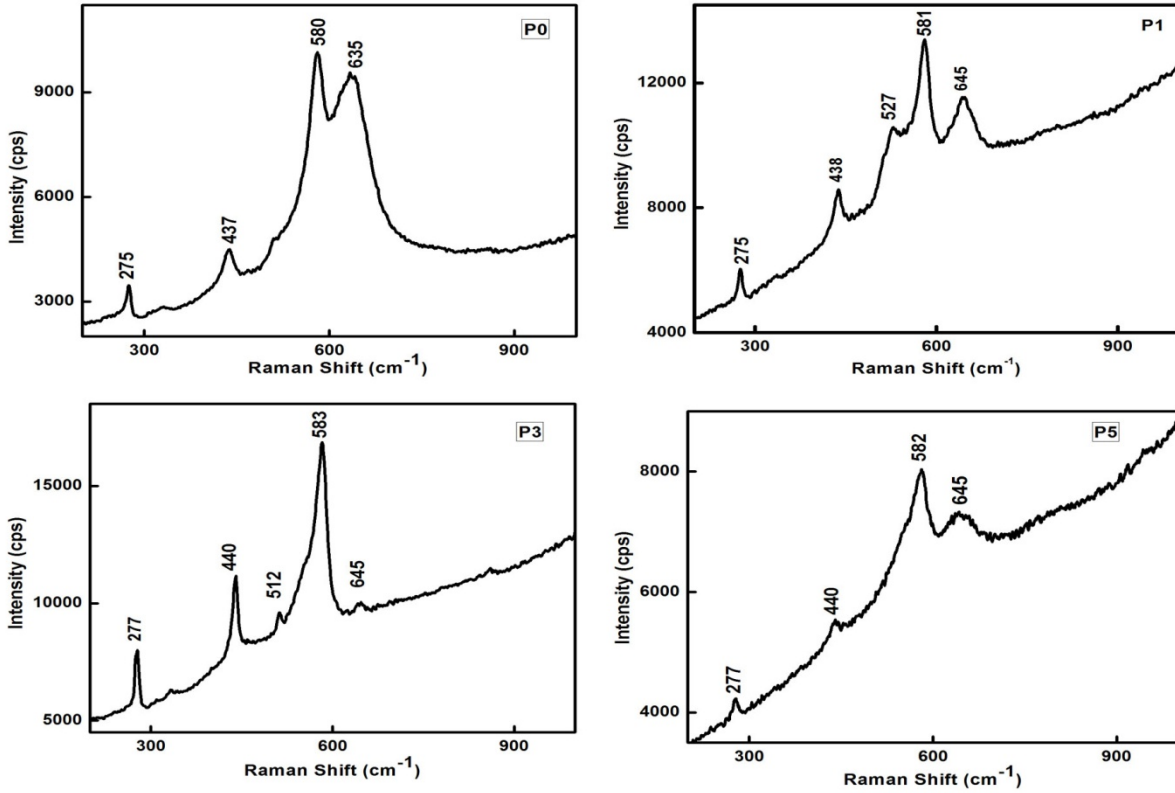


Fig. 2 Micro-Raman spectra of undoped and Pr doped ZnO films with doping concentrations 0, 1, 3 and 5wt%.

The Raman spectra of the undoped and PrdopedZnOfilms are shown in Fig. 2. The most intense Raman band at 580 cm^{-1} in the Raman spectrum of pure ZnO film can be due to the longitudinal optical phonon $E_1(LO)$ mode, which is caused by the formation of defects such as oxygen vacancy or interstitial zinc in ZnO [48, 49]. The medium intense band at 437 cm^{-1} in the Raman spectrum corresponds to ZnO non polar optical phonon $E_2(\text{high})$ mode, which is the intrinsic characteristic of hexagonal wurtzite structure of ZnO [50]. The $E_2(\text{high})$ mode is mainly associated with the vibration of the lighter oxygen sub-lattice. The Raman spectrum presents an intense band at 645 cm^{-1} and a medium intense band at 275 cm^{-1} . These additional modes may be related to intrinsic host lattice defects such as oxygen vacancies and zinc interstitials etc. Duet *al.* also observed additional phonon modes at 275 and 645 cm^{-1} in Mn, Co-doped films and they attributed these additional modes to defect states such as oxygen vacancies and zinc interstitials induced by impurity doping [51, 52]. Certain authors report the appearance of Raman bands in the 250-300 cm^{-1} region due to the activation of silent modes [48, 53].

The Raman spectrum of 1 wt% Pr doped film presents two intense Raman bands at 581 and 645 cm^{-1} and medium intense Raman bands at 438, 527 and 275 cm^{-1} . The Raman spectrum of 3wt% Pr doped ZnO film presents a very intense band at 583 cm^{-1} , intense Raman bands at 440 and 277 cm^{-1} and two weak bands at 512 and 645 cm^{-1} . An enhancement in intensity of the bands at 440, 277 and 581 cm^{-1} is observed in the Raman spectrum of the P3 film

compared to other films. Also the band at 645 cm^{-1} in this film presents the lowest intensity among the films. The observation of sharper bands and reduction in intensity of the defect related band at 645 cm^{-1} in the Raman spectrum of P3 film compared to that of the other films is an indication of enhanced crystalline quality of the P3 film, supporting the XRD findings. In the Raman spectrum of 5wt% Pr doped ZnO film, the bands are broader and less intense compared to that of the other films which can be due to the enhanced strain introduced due to high Pr doping. It is also seen that the intensity of $E_2(\text{high})$ mode is less compared to that of $E_1(\text{LO})$ mode in all the films, indicating the presence of defects in the undoped and Pr doped films in spite of the c-axis orientation observed from the XRD patterns.

The position of $E_1(\text{LO})$ mode shows a blue shift with Pr doping. In the undoped film $E_1(\text{LO})$ mode appears at 580 cm^{-1} , whereas in P1 and P3 films it is observed at 581 and 583 cm^{-1} respectively. In P5 film, it appears at 582 cm^{-1} as a broad band with less intensity. Ye *et al.*, attributed the origin of this blue shift in the Raman spectra of ZnO films to the residual stress along the c-axis due to the effect of oxygen deficiency [54]. The position of $E_2(\text{high})$ mode is also found to be shifting towards higher wave numbers in the Pr doped films. In the undoped film $E_2(\text{high})$ is observed at 437 cm^{-1} , whereas in P1 and P3 films it is observed at 438 and 440 cm^{-1} respectively. In the P5 film $E_2(\text{high})$ is observed at 440 cm^{-1} as a broad feature with very less intensity. The position of $E_2(\text{high})$ mode in wurtzite structure is highly influenced by the residual stress in the film. An increase in $E_2(\text{high})$ frequency is ascribed to compressive stress, whereas a decrease in $E_2(\text{high})$ frequency is ascribed to tensile stress [55, 56]. Therefore the blue shift in the $E_2(\text{high})$ frequency with respect to the bulk value of 437 cm^{-1} indicates the presence of compressive stress in the films. This argument is consistent with the XRD findings that compressive stress is acting in the films.

The surface morphology of the films was characterized with atomic force microscope (AFM) in contact mode. (Fig. 3.)

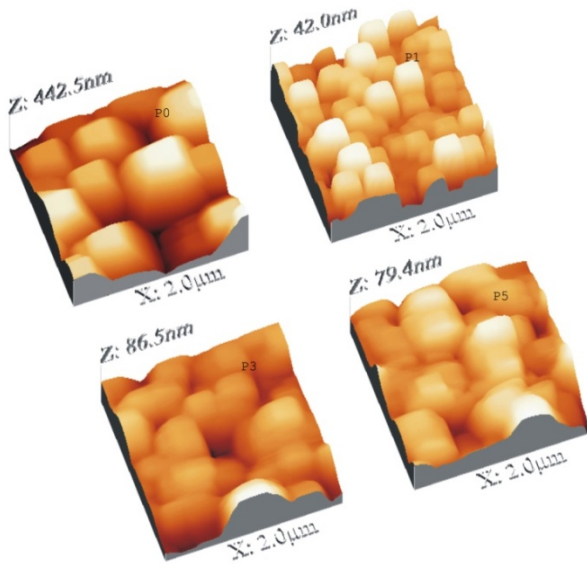


Fig. 3 (a)

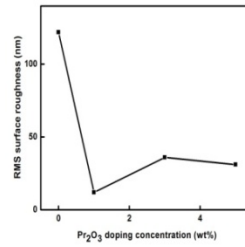


Fig. 3 (b)

Fig. 3 (a) AFM micrographs of undoped and Pr doped ZnO films with doping concentrations 0, 1, 3 and 5 wt% and 3(b) variation of RMS surface roughness with Pr doping concentration.

The microstructure of the films consists of large grains with well-defined grain boundaries showing the good crystalline nature in the films. There is a tendency of agglomeration of grains in films with higher Pr doping concentration. The rms roughness of the films is measured from the AFM micrographs. The undoped film shows the highest value (~122 nm) for rms roughness, whereas the 1 wt% doped film shows the least value (~12 nm) for rms roughness. The doped films present lesser rms roughness compared to the undoped film. The variation of rms roughness with Pr doping concentration is shown in Fig. 3.b.

The SEM micrographs of pure and 5 wt% Pr doped ZnO films are shown in Fig. 4.

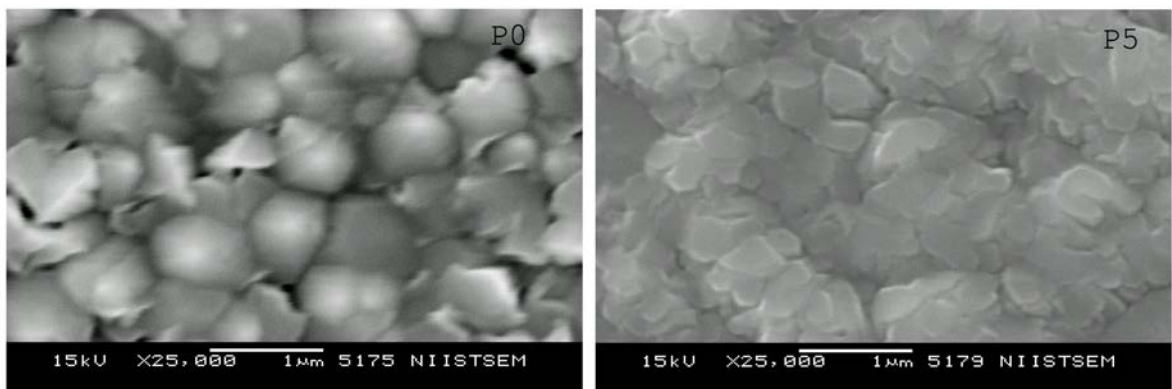


Fig. 4 SEM micrographs of undoped and 5 wt% Pr doped ZnO films.

These images reveal the presence of densely packed larger grains supporting the good crystalline nature of the films. The SEM micrograph of 5 wt% Pr doped film shows a tendency of agglomeration as observed in the AFM analysis.

The chemical composition of the undoped and 5wt% PrdopedZnO films were investigated by EDX analysis (Fig. 5). The analysis shows the presence of prominent peaks for Zn and oxygen, suggesting the formation of ZnO phase in the film. The presence of peak corresponding to praseodymium in the EDX spectrum of 5wt% PrdopedZnO film indicates the incorporation of Pr^{3+} in the doped film.

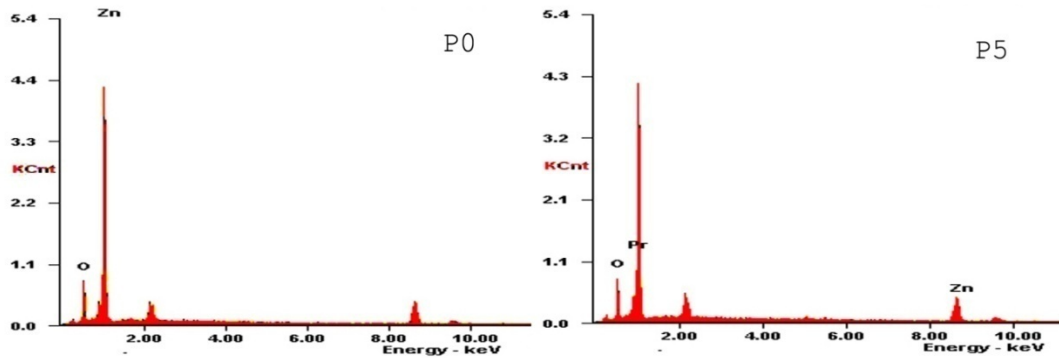


Fig. 5 EDX spectra of undoped and 5 wt% Pr doped ZnO films.

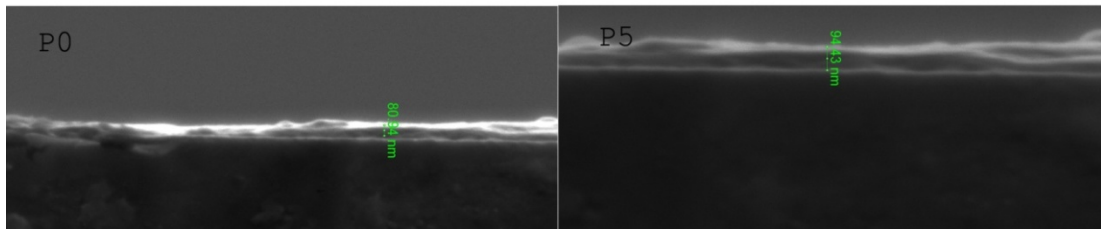


Fig. 6 Cross-sectional SEM micrographs of undoped and 5 wt% Pr doped ZnO films showing thickness of the samples.

The thickness measurements of the P0 and P5 films were carried out using lateral SEM measurements (Fig. 6.) and the thickness is found to be 80 and 94 nm respectively. The thickness measurements were also carried out using Dektak 6M stylus profile meter and the thickness of the films is found to vary between 70 – 78 nm (Table.1).

The optical transmission spectra of the undoped and Pr doped ZnO films were recorded in the wavelength range of 300- 900 nm and are shown in Fig. 7. The undoped film shows an average transmittance below 60% in the 400 to 900nm region. It can be seen that the doped films show very high transmittance above 80% in the 400 to 900 nm region. 1 and 3wt% Pr doped ZnO films show average transmittance above 90%.

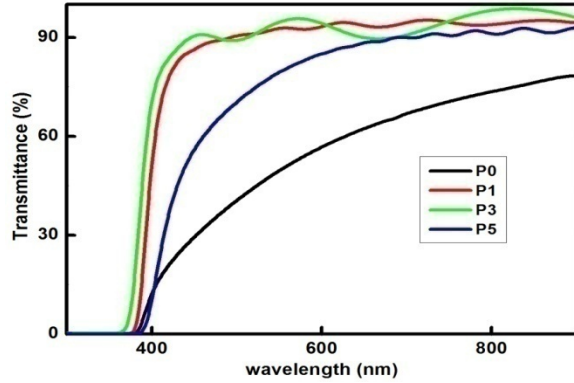


Fig. 7 Transmittance spectra of undoped and Pr doped ZnO films with doping concentrations 0,1,3 and 5 wt%.

Thus the transmittance spectra for the moderately doped films show excellent optical transparency in the visible and near IR spectral region, which plays an important role for the potential applications in transparent optoelectronic devices. The slight reduction in transparency of 5wt% Pr doped ZnO films compared to that of the 1 and 3 wt% Pr doped ZnO films is an indication of the decline in crystallinity of the film as evident from XRD and Raman analysis. The oscillations in the transmission spectra of the doped films are caused by optical interference arising due to difference in refractive index of films with substrate and the interference of multiple reflections originated from film and substrate surfaces. This confirms the formation of smooth transparent films having uniform thickness on quartz substrate [57, 58, 59].

The optical transmittance of the film is found to depend on surface morphology and is found to be increasing with decrease in surface roughness due to the reduction in scattering losses. The observed low transmittance for the undoped film can be due to its high value of rms surface roughness. From the optical spectra, Tauc plots were constructed (Fig. 8) to obtain the values of band gap energies of the films. The optical band gap of the direct band gap semiconductor can be determined by plotting $(\alpha h\nu)^2$ versus $(h\nu)$ and extrapolating the linear region of the plot to zero absorption ($\alpha = 0$) [60]. Undoped ZnO films show a band gap of 2.94 eV, whereas the P1, P3 and P5 films show band gap energies of 3.02, 3.06 and 2.96 eV respectively.

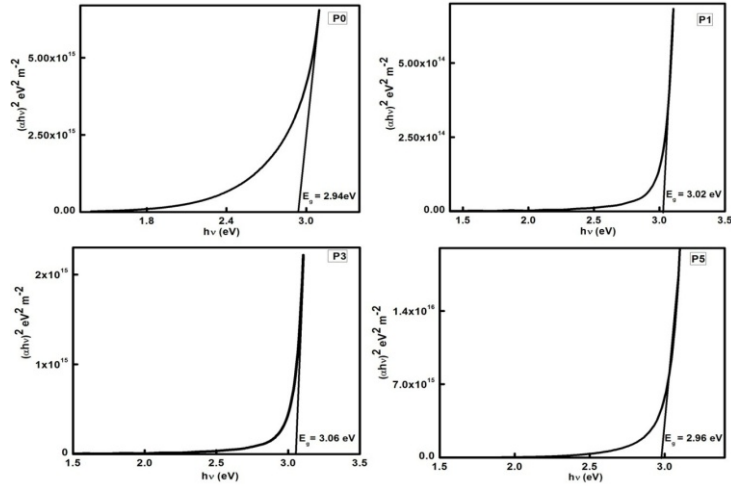


Fig. 8 Tauc plots of undoped and Pr doped ZnO films with doping concentrations 0,1, 3 and 5 wt%.

The band gap energy of ZnO film is found to be influenced by different factors such as crystalline quality of the film, grain size, strain, influence of dopant, defects etc. [61]. The blue-shift of absorption edge of a degenerate semiconductor with an increase in carrier concentration is expected in doped semiconductors, which is known as Burstein–Moss (BM) effect. ZnO being typically an n-type semiconductor, the Fermi level of heavily doped ZnO would be located near the conduction band edge. The origin of BM shift due to doping can be attributed to the charge carriers generated by the valence difference between the dopant and host cations. Oxygen vacancy is another probable candidate to cause BM effect [62, 63, 64]. The shift in band gap may occur due to stress induced distortion of the band by substrate film interaction and also due to compositional variation [62, 65, 66, 67]. Wan et al., reported that stress fields modulate the band gap and band structure of GaN films and thereby modifying the optical properties of the devices [68, 69]. Huang *et al.* reported that a tensile strain produces a decrease in band gap whereas a compressive strain can result in an increase in band gap. [70, 71]. Renet *al.*, suggested that higher defect concentrations in the film contribute to higher energy absorption edges [72]. It is found that the band gap energy of the P1 and P3 films are blue shifted with Pr doping. But the band gap energy shows a reduction in heavily doped film (P5). The observed variation of band gap energy with Pr doping can be attributed to the combined effect of BM effect, strain and defects in the films.

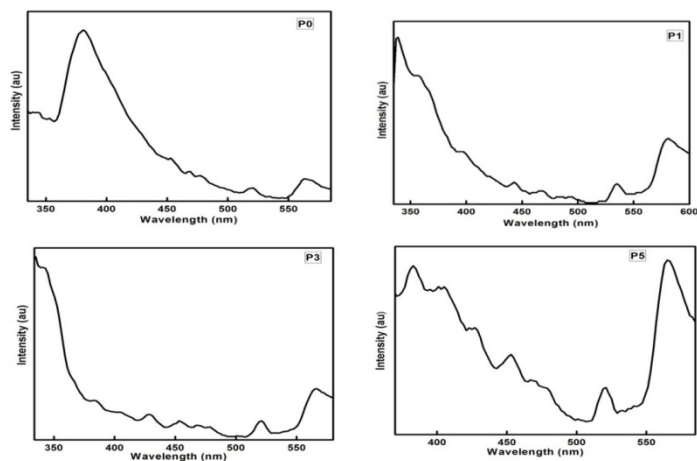


Fig. 9 Photoluminescence spectra of undoped and Pr doped ZnO films with doping concentrations 0,1,3 and 5 wt%.

Fig.9 represents the room temperature photoluminescence (PL) spectra of the undoped and praseodymium doped ZnO films excited by 325 nm. All the samples show UV and visible emission. The near band edge (NBE) ultra violet emission comes from the free excitonic emission of ZnO arising due to the radiative transition from near the conduction band edge to the valance band [73] and the medium intense emissions in the visible region are due to the deep level emissions caused by the defects such as oxygen vacancy, Zn interstitials etc.[74]. Hong *et al.*, reported that the intensity of the UV emission, which is the characteristics of ZnO films, strongly depend on crystallinity and stoichiometry of the films. The visible emission originates from defects such as oxygen vacancy, zinc interstitials etc. [75]. The PL spectrum of undoped film shows a strong UV emission~ 380 nm and weak emission ~520 and 565 nm. In the doped films the intensity of the defect related peaks enhances. Ilanchezhian et al. also observed increase in visible luminescence with Pr doping [28]. They attributed this to the increase in native defects due to doping and suggested that when Pr^{3+} replaces Zn^{2+} , oxygen defects are generated to maintain charge neutrality.

The intensity of these peaks in P3 film is the lowest among the doped films which is consistent with the XRD and Raman findings that P3 film has the highest degree of crystallinity among the doped films investigated. Interestingly the intensity of the defect related peaks is the highest in P5 film where the crystallinity is the lowest as evidenced by XRD and Raman analysis.

The PL intensity of the films depends on the surface morphology. The films with highest rms surface roughness show enhanced PL intensity due to the scope for strong absorption of incident light due to its increased surface area. A rough film can allow the incident light to be reflected into another portion of the film surface. This can lead to more efficient use of the excitation energy and hence superior PL intensity [76]. The undoped film with the highest value of rms surface roughness shows the highest PL intensity for NBE.

The visible emission in ZnO in the blue region (445 nm) is generally attributed to the transition between zinc interstitial defect centre (Zn_i) and oxygen interstitial (O_i) in ZnO [77]. The origin of green luminescence in ZnO is still unclear. Different explanations are proposed by many researchers to reveal the mechanism of green emission in ZnO. Many authors attributed the origin of green emission in ZnO to the oxygen vacancy [78, 79, 80] Mondalet *al.*, reported that the green emission in ZnO is generally attributed to the recombination of photo generated hole with singly ionized oxygen vacancies [81]. Vanheusdenet *al.* also suggested that the ionized oxygen vacancies are responsible for green emission in ZnO [82, 83]. Lin *et al.*, suggested that green emission corresponds to electron transition from the bottom of the conduction band to an oxide antisite defect level (O_{Zn}) [84]. Roy *et al.*, and Li *et al.*, reported that the green emission in ZnO depends on fabrication conditions [85, 86]. The defect levels in ZnO calculated using full-potential muffin –tin orbital (FP-LMTO) method by Sun shows that the energy interval between the bottom of the conduction band and the antisite defect level (O_{Zn}) is 2.38 eV [87, 88]. Therefore the green emission observed in our films can be attributed to antisite defect level (O_{Zn}) as observed by Lin *et al.* [84].

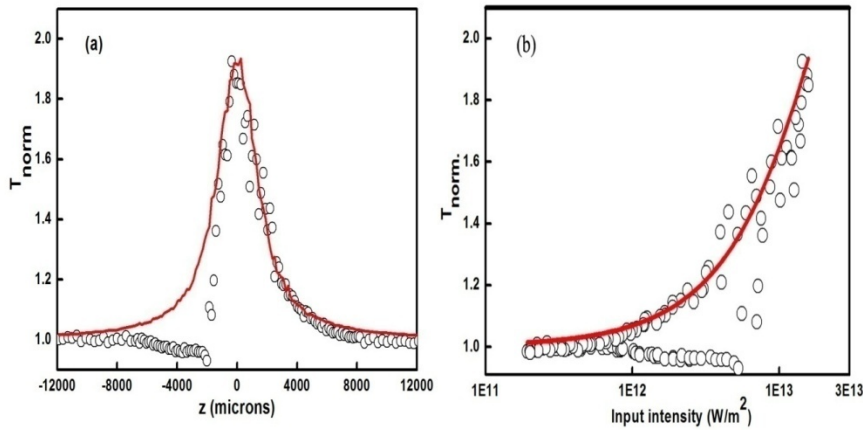


Fig. 10 (a) Open aperture Z-scan curve and (b) fluence vs. normalized transmittance of the 1 wt% Pr doped ZnO films. Circles represent the measured data and solid curves show the numerical fit.

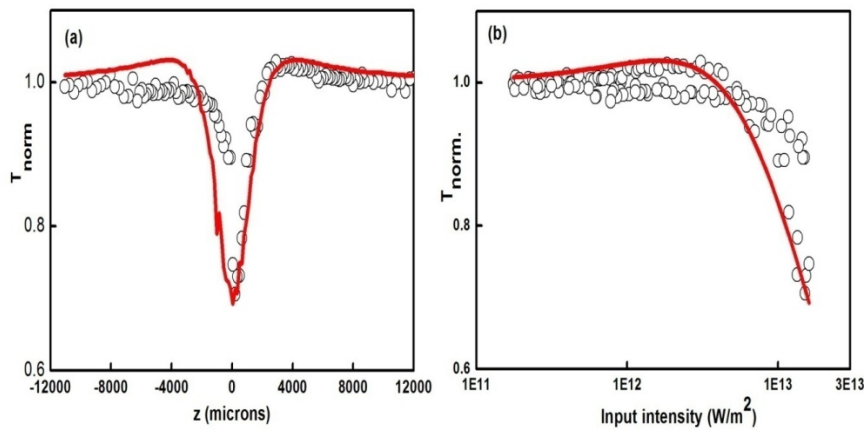


Fig. 11 (a) Open aperture Z-scan curve and (b) fluence vs. normalized transmittance of the 5 wt% Pr doped ZnO films. Circles represent the measured data and solid curves show the numerical fit.

A nonlinear absorption is a nonlinear change, either increase or decrease in absorption with increase in intensity of the incident light. This can be of two types viz; saturable absorption (SA) and reverse saturable absorption (RSA). With increasing intensity, if the excited states show saturation owing to their long lifetimes, the transmission will show saturable absorption behavior. If the excited state has strong absorption compared with that of the ground state, the transmission will show reverse saturable absorption behavior [30, 89]. Earlier reports show that ZnO exhibits second and third-order nonlinear optical behavior, both in single crystals and in thin films [90]. Many researchers have investigated the effect of dopants on the non-linear optical behavior of ZnO. Karthikeyan *et al.*, has reported the value of the order of 10^{-13}mW^{-1} for Na doped ZnO [91], Vinodkumar *et al.*, has obtained the value of $6 \times 10^{-7} \text{mW}^{-1}$ for Cd doped ZnO films [92] and Kumari *et al.*, has reported the value of the order of 10^{-6}cmW^{-1} for Er doped ZnO films [16].

Nonlinear optical properties of 1 and 5 wt% Pr incorporated ZnO nanostructures have been investigated by the open aperture Z-scan technique [93]. The variations of normalized transmittance exhibited by the 1 wt% Pr doped ZnO film as a function of distance and input fluence are shown in Fig. 10(a) and (b) respectively. The corresponding curves for the 5 wt% Pr doped ZnO film are shown in Fig. 11(a) and (b) respectively.

The 1 wt% Pr doped ZnO film shows a normalized transmittance peak at the beam focus, indicating a negative nonlinear absorption due to saturable absorption (SA) [94, 95]. However, the 5 wt% Pr doped ZnO film exhibits a strong positive nonlinear absorption due to reverse saturable absorption (RSA) [89].

In semiconductors, heat energy tends to reduce the Fermi level resulting in an increase in the number of carriers in the conduction band. This depletes the ground level and induces bleaching in the ground state absorption leading to saturable absorption [96]. Irimpan *et al.* reported that the non-linear behavior of ZnO is very sensitive to impurities and native defects and suggested that the mechanism behind the saturable absorption can be due to the saturation of linear absorption of defect states in ZnO [96]. In RSA, the molecules in the ground state and excited states can absorb the incident photons of the same wavelength and the absorption of excited states will be larger than that of the ground state. Hence the transmission decreases with increase in intensity [95]. The drastic variation of optical nonlinearity with respect to Pr doping concentration may be due to the changes in various properties induced by Pr doping such as defect state density, morphology and particle size. Pr doping can create defect centers in ZnO lattice as revealed by Raman analysis. These defect centers can act as photon-trapping states over the surface. In semiconductor nanocrystals, the surface chemistry of the localized trapping states is responsible for the optical nonlinear properties [89]. If the linear absorption cross-section of the trap states is higher than the ground state, then direct excitation from these surface-trapped states will promote the photocarriers to higher energy levels in the nanocrystal, giving rise to the optical nonlinearity. The nonlinear optical response of trapped states also depends on the density and lifetime of trapped states [89, 97, 98].

In the present case the nonlinear absorption coefficient $\alpha(I)$ can be expressed by the following relation [99]

$$\alpha(I) = \frac{\alpha_0}{1 + \left(\frac{I}{I_s}\right)} + \beta I \quad (6)$$

where the saturation intensity I_s is defined as the input intensity at which the absorption reduces to half of the linear absorption, α_0 is the unsaturated linear absorption coefficient at the wavelength of excitation, and I is the input intensity. β is the effective non-linear absorption coefficient.

For a given input intensity, the transmitted intensity can be calculated by numerically solving the propagation equation given by

$$\frac{dI}{dz} = - \left[\left(\frac{\alpha_0}{1} + \left(\frac{I}{I_s} \right) \right) + \beta I \right] I \quad (7)$$

Here z indicates the propagation distance within the sample. The I_s and β values are obtained by numerically fitting Equation 10 to the experimental data given in Figures 10b and 11b. For P1 film the I_s value is found to be $1 \times 10^{13} \text{ Wm}^{-2}$. The value of β for 5wt% Pr doped film is found to be $0.7 \times 10^{-10} \text{ mW}^{-1}$, and the saturation intensity is found to be $4 \times 10^{12} \text{ Wm}^{-2}$.

It is interesting to note that while 1wt% Praseodymium incorporated ZnO shows saturable absorption, the 5wt% Praseodymium incorporated ZnO shows reverse saturable absorption. The switch over from saturable absorption to reverse saturable absorption is an interesting effect that can be utilized for optical switching, optical pulse compression and laser pulse narrowing. The change over in sign of the non-linearity is related to the interplay of exciton band bleach and optical limiting mechanisms [100]. In semiconductors, RSA results mainly due to the nonlinear mechanisms such as two-photon absorption (TPA), free-carrier absorption (FCA), nonlinear scattering or a combination of these processes [95, 101]. In semiconductors, two-photon absorption is allowed when the incident light source energy is less than the direct band gap energy E_g , but greater than $E_g/2$. For $\frac{1}{2} E_g < h\omega < E_g$ the nonlinear response involves virtual processes and the two photon process is much stronger than the one-photon process [95, 101]. TPA is one of the important basic mechanisms for induced absorption. Sekeret *al.*, reported that during excited state absorption, the non-linear process dominates. The first excited state electron in the lower conduction band region is excited to the higher excited state in the conduction band region by absorbing a second photon. Such a process is known as free carrier absorption [102].

The change in non-linear optical behavior in semiconductors may originate from different factors such as defect state density, morphology, quantum confinement etc. [30]. The optical limiting property observed in P5 film can be due to the enhancement in defect densities due to higher doping concentration of Pr. The Raman spectral analysis of the films show that at higher doping concentrations, the $E_1(LO)$ mode is more prominent and the $E_2(\text{high})$ mode becomes very weak. This may be due to the formation of defects such as oxygen vacancies and zinc interstitials etc introduced by Pr doping. Hence in 5wt% Pr doped ZnO film, in addition to TPA, the presence of defect states also may have contribution to the change of non-linear absorption behavior from SA to RSA. The presence of defects in the films for optical limiting behavior in MoO_3 films was reported by Navaset. *al.* [30]. The

high value of non-linear absorption coefficient (β) for 5wt% Pr doped ZnO film suggests the suitability of Pr₂O₃ doped ZnO films for optoelectronic device applications owing to their good non-linear response.

4. Conclusion

The structural, optical and spectroscopic investigations of Pr doped ZnO films reveal that the dopant concentration has a profound effect on its structural, optical and non-linear optical properties. The XRD and Raman analysis reveals the presence of hexagonal wurtzite ZnO crystalline phase in the films. From the optical spectroscopic analysis it is found that Pr doping enhances the transparency of the films. A green emission is observed in all the films and its intensity increases with increase in Pr concentration. As the Pr doping concentration increases, the non-linear absorption behavior switches from SA to RSA.

Acknowledgements

Authors wish to thank UGC-DAE CSR, Indore for Micro-Raman measurements and Dr. Reji Philip, Raman Research Institute, Bangalore for open aperture Z-scan measurements.

References

- [1] R. Sreeja, Jobina John, P.M. Aneesh, M.K. Jayaraj, *Optics Communications* 283 (2010) 2908–2913.
- [2] Y. W. Heo, D. P. Norton, and S. J. Pearton, *J. Appl. Phys.* 98 (2005) 073502; DOI: 10.1063/1.2064308.
- [3] Yuxin Wang, Xinyong Li, Guang Lu, XieQuan, Guohua Chen, *J. Phys. Chem. C* 112 (2008) 7332–7336.
- [4] K Mirabbaszadeh, M Mehrabian, *Phys. Scr.* 85 (2012) 035701 (8pp), DOI:10.1088/0031-8949/85/03/035701.
- [5] Jun-ichi Nomoto, Tomoyasu Hirano, Toshihiro Miyata, Tadatsugu Minami, *Thin Solid Films* 520 (2011) 1400–1406. doi:10.1016/j.tsf.2011.10.003.
- [6] Won Il park, Gyu-Chul Yi, *Adv. Mater.* 16 (2004) 87–90. Doi:10.1002/adma.200306052.
- [7] Kieun Seong, Kyongjun Kim, Si Yun Park, Youn Sang Kim, *Chem. Commun.*, 49(2013) 2783–2785. DOI: 10.1039/c3cc38021a.
- [8] S.J. Pearton, D.P. Norton, Y.W. Heo, L.C. Tien, M.P. Ivill, Y. LI, B.S. Kang, F. Ren, J. Kelly, A.F. Hebard, *Journal of Electronic Materials*, Vol. 35, No. 5 (2006) 262–268.
- [9] W.Q. Zou, C.N. Ge, G. Venkataiah, H. L. Su, H.L.Hsu, J.C.A.Huang, X.C. Liu, F.M.Zhang, Y.W.Du, *J. Appl. Phys.* 111, 113704 (2012).
- [10] A. Cetin, R. Kibar, M. Ayvacikli, Y. Tuncer, Ch.Buchal, P.D. Townsend, T. Karali, S.Selvi, N. Can, *Surface Coating Technology* 201 (2007) 8534–8538.
- [11] Y. Caglar, S. Ilican, M. Caglar, F. Yakuphanoglu, *J.Sol-Gel Sci.Technol* 53 (2010) 372. DOI: 10.1007/s10971-009-2105-0.
- [12] Kuo-Feng Lin, Hsin-Ming Cheng, Hsu-Cheng Hsu, Li-Jiaun Lin, Wen-Feng Hsieh, *Chemical Physics Letters* 409 (2005) 208–211.

- [13] Shubra Singh, P. Thiagarajan, K. Mohan Kant, D. Anita, S. Thirupathiah, N. Rama, BrajeshTiwari, M. Kottaisamy, M S RamachandraRao, *J. Phys. D: Appl. Phys.* 40 (2007) 6312–6327, DOI:10.1088/0022-3727/40/20/S15.
- [14] Y.C. Liu, S.K. Tung, J.H. Hsieh, *Journal of Crystal Growth* 287 (2006) 105–111.
- [15] A. Ohtomo, K. Tamura, M. Kawasaki, T. Makino, Y. Segawa, Z. K. Tang, G. K. L. Wong, Y. Matsumoto, H. Koinuma, *Applied Physics Letters* 77, (2000) 2204-2206; DOI: 10.1063/1.
- [16] VinayKumari, Vinod Kumar, B.P. Malik, R.M. Mehra, Devendra Mohan, *Optics Communications* 285 (2012) 2182–2188.
- [17] Shu-Man Liu, Feng–Qi Liu, Zhan-Guo Wang, *Chemical Physics Letters*, 343, (2001) 489-492.
- [18] Naoki Wakiya, Sung-Yong Chun, Kazuo Shinozaki, and NobuyasuMizutani, *Journal of Solid State Chemistry* 149, (2000) 349-353 DOI:10.1006/jssc.1999.8543.
- [19] Kaipeng Liu, Beifang Yang, Hongwei Yan, Zhengping Fu, Meiwang Wen, Youjun Chen and JianZuo, *Journal of luminescence*, 129 (2009) 969-972.
- [20] B.J. Jin, S. Im, S.Y.Lee, *Thin Solid Films* 366 (2000) 107-110.
- [21] H. Deng, J.J.Russell ,R.N.Lamb, B.Jiang, Y.Li, X.Y.Zhou, *Thin Solid Films* 458 (2004) 43–46.
- [22] Yi Li, W.V. Youdclis, B.S. Chao and H. Yamauchi, *J. Am. Ceram Soc.*, 76 (12) 1993, 2985-2992.
- [23] HaoshuangGu, DinghuaBao, Shimin Wang, DongfaGao, AnxiangKuang, Xingjiao Li, *Thin Solid Films*, 283 (1996) 81-83.
- [24] Yoshihiro Inoue, Yoichi Okamoto, Jun Morimoto, *J Mater Sci* (2008) 43:368–377, DOI 10.1007/s10853-006-1314-y.
- [25] Yukio Sato, TeruyasuMizoguchi, Fumiyasu Oba, Masatada Yodogawa, Takahisa Yamamoto, Yuichi Ikuhara, *Appl. Phys. Lett.*, Vol. 84, No. 26, 2004.
- [26] Jose Geraldo de Melo Furtado, Luiz Antonio Saleh, Eduardo Torres Serra, Gloria Suzana Gomes de Oliveira, Maria Cecilia de SouzaNobrega, *Materials Research*, Vol. 8, No. 4, (2005) 425-429.
- [27] AlirezaKhataee, AtefehKarimi, Samira Arefi-Oskoui, Reza DarvishiCheshmehSoltani, YounesHanifehpour, BehzadSoltani, Sang Woo Joo, *UltrasonicsSonochemistry* 22 (2015) 371–381.
- [28] P. Ilanchezhian, G. Mohan Kumar, M. Subramanian, R. Jayavel, *Materials Science and Engineering B* 175 (2010) 238–242.
- [29] Yukio Sato, Fumiyasu Oba, Masatada Yodogawa, Takahisa Yamamoto, Yuichi Ikuhara, *Journal of Applied Physics* 95, (2004) 1258. DOI: 10.1063/1.1636816.
- [30] NavasIllyaskutty, SreejaSreedhar, Heinz Kohler, RejiPhilip, VinodkumarRajan, V. P. MahadevanPillai, *J. Phys. Chem. C*. 117 (2013) 7818–7829. dx.doi.org/10.1021/jp311394y.
- [31] S. Maniv, W.D. Westwood, E. Colombini, *J. Vac. Sci. Technol.* 20 (1982) 162.
- [32] R. Vinodkumar, I. Navas, K. Porsezian, V. Ganesan, N.V. Unnikrishnan, V.P. MahadevanPillai, *SpectrochimicaActa Part A: Molecular and Biomolecular Spectroscopy* 118 (2014) 724–732.
- [33] J. Mass, P. Bhattacharya, R.S. Katiyar, *Materials Science and Engineering B*103 (2003) 9-15.

- [34] Minrui Wang, Jing Wang, Wen Chen, Yan Cui, Liding Wang, *Materials Chemistry and Physics* 97 (2006) 219–225.
- [35] Y. F. Li, B. Yao, Y. M. Lu, C. X. Cong, Z. Z. Zhang, Y. Q. Gai, C. J. Zheng, B. H. Li, Z. P. Wei, D. Z. Shen, X. W. Fan, L. Xiao, S. C. Xu, Y. Liu, *Applied Physics Letters* 91, (2007) 021915. DOI: 10.1063/1.2757149.
- [36] Remadevi Sreeja Sreedharan, Vedachalaiyer Ganesan, Chellappan Pillai Sudarsanakumar, Kaushalkumar Bhavsar, Radhakrishna Prabhu, Vellara Pappukutty Pillai Mahadevan Pillai, *Nano Reviews* 2015, 6:26759, DOI: <http://dx.doi.org/10.3402/nano.v6.26759>.
- [37] T. Ohshima, R.K. Thareja, T. Ikegami, K. Ebihara, *Surface and Coatings Technology*, 169 –170 (2003) 517–520.
- [38] Bhaskar Chandra Mohanty, YeonHwa Jo, Deuk Ho Yeon, IkJin Choi, Yong Soo Cho, *Appl. Phys. Lett.* 95 (2009) 062103. DOI: 10.1063/1.3202399.
- [39] P. M. Verghese and D. R. Clarke, *Journal of Applied Physics* 87, (2000) 4430. DOI: 10.1063/1.373088.
- [40] O. Kappertz, R. Drese and M. Wuttig *Journal of Vacuum Science & Technology A*20, (2002) 2084. DOI: 10.1116/1.1517997.
- [41] Robert J. Drese and Matthias Wuttig, *Journal of Applied Physics* 98 (2005) 073514. DOI: 10.1063/1.2061888.
- [42] B.D Cullity, *Elements of X-ray Diffractions*, Addison-Wesley, Reading, MA, 1978. p. 102.
- [43] S.Ilican, Y.Caglar, M. Caglar, *J.Optoelectronics and Advanced materials*, Vol. 10, No. 10,(2008), 2578 – 2583.
- [44] Bingqiang Cao, Weipingcai, Haibo Zeng and Guotao Duan, *J. Appl. Phys.* 99 (2006) 073516.
- [45] W. G. Fateley, F.R.Dollish, N.T.McDevitt and F.F.Bentley, “Infrared and Raman Selection rules for molecular and lattice vibrations- The Correlation Method” Wiley, New York, 1966.
- [46] T. Zhang, Y. Zeng, H. T Fan, L. J. Wang, R. Wang, W. Y. Fu, H. B. Yang, *J. Phys. D: Appl. Phys.* 42 (2009) 045103 , <http://dx.doi.org/10.1088/0022-3727/42/4/045103>.
- [47] M. Koyano, Phung Quocbao, le Thi Thanhbinh, Le Hongha, Nguyen Ngoclong, Shinichi Katayama, *phys. Stat. sol (a)* No.1 (2002) 125-131.
- [48] M. Tzolov, N. Tzenov, D. Dimova-Malinovska, M. Kalitzova, C. Pizzuto, G. Vitalic, G. Zolloc, I. Ivanov, *Thin Solid Films* 379 (2000) 28-36.
- [49] A. K. Pradhan, Kai Zhang, G. B. Loutts, U. N. Roy, Y. Cui, A. Burger, *J. Phys.: Condens. Matter* 16 (2004) 7123–7129. DOI:10.1088/0953-8984/16/39/043.
- [50] Linhua Xu, Linxing Shi, Xiangyin Li, *Applied Surface Science* 255 (2009) 5957-5960.
- [51] C.L. Du, Z.B. Gu, M.H. Lu, J.Wang, S.T. Zhang, J. Zhao, G.X. Cheng, H.Heng, Y.F. Chen, *J.Appl.Phys.*99, (2006) 123515 DOI: 10.1063/1.2208298.
- [52] C. Bundesmann, N. Ashkenov, M. Schubert, D. Spemann, T. Butz, E. M. Kaidashev, M. Lorenz, M.Grundmann. *Applied Physics Letters*,83 (2003) 1974.DOI: 10.1063/1.1609251.

- [52] J. M. Calleja, M. Cardona, *Phys. Rev. B: Solid State*, 16 (1977) 3753.
- [53] K. McGuire, Z. W. Pan, Z. L. Wang, D. Milkie, J. Menéndez and A. M. Rao, *J. Nanosci. Nanotech.* 2 (2002) 1–4.
- [54] Jiandog Ye, ShulinGu, Shunmin Zhu, Tong Chen, Wei Liu, Feng Qin, Liqun Hu, Rong Zhang, Yi Shi and YoudouZheng, *J. Vac. Sci. Technol. A* 21(4), (2003) 979-982. DOI: 10.1116/1.1580836.
- [55] Ji Nan Zeng, Juay Kiang Low, Zhong Min Ren, Thomas Liew, Yong Feng Lu, *Applied Surface Science*, 197-198 (2002) 362-367.
- [56] Yanqiu Huang, Meidong Liu, Zhen Li, YikeZeng, Shaobo Liu, *Materials Science and Engineering B* 97 (2003)111-116.
- [57] Swanepoel. R. *J. Phys.E: Sci. Instrum.* 17 (1984) 1214–22.
- [58] R. Jolly Bose, R. Vinod Kumar, S. K. Sudheer, V. R. Reddy, V. Ganesan, V. P. Mahadevan Pillai, *J. Appl. Phys.* 112 (2012) 114311. <http://dx.doi.org/10.1063/1.4768206>.
- [59] K. J. Lethy, D. Beena, R. Vinodkumar, V. P. Mahadevan Pillai, V. Ganesan, V. Sathe, D. M. Phase, *Appl. Phys. A* 91 (2008) 637-649.
- [60] Pradipta K Nayak, Jinwoon Kim, seungjun Chung, Jaewookjeong, Changhee Lee and Yongtaek Hong, *J. Phys. D: Appl. Phys.* 42(2009) 035102(6pp). DOI:10.1088/0022-3727/42/13/139801.
- [61] TingtinRen, Holly R. Baker, Kristin. M. poduska, *Thin Solid Films*, 515 (2007) 7976-7983.
- [62] Somnath. C. Roy, G.L. Sharma, M.C. Bhatnagar, *Solid State Communications* 141 (2007) 243-247.
- [63] Y.G. Wang, S.P. Lau, H.W. Lee, S.F. Yu, B.K. Tay, X.H. Zhang, K.Y. Tse, H.H. Hng, *J. Appl. Phys.*, 94 (2003) 1597.
- [64] W.L. Wang, J.Y. Gao, K.J. Lao, D.L. Peng, S.R. Jiang, *Matter. Lett.* 13 (1992) 342.
- [65] R. Thomas, D.C. Dube, M.N. Kamalasanan, S. Chandra, *Thin Solid Films*, 346 (1999) 212.
- [66] R. Thielsch, K. Kaemmer, B. Holzapfel, L. Schultz, *Thin solid Films*, 301, (1997) 203.
- [67] R. Vinodkumar, K.J. Lethy, D. Beena, A.P. Detty, I. Navas, U.V. Nayar, V.P. Mahadevan Pillai, V. Ganesan b, V.R. Reddy, *Solar Energy Materials & Solar Cells* 94 (2010) 68–74.
- [68] Keshu Wan, Alessandro Alan Porporati, GanFeng, Hui yang, Giuseppe Pezzotti, *Applied Physics Letters*, 88 (2006) 251910-3.
- [69] A. Abdolazadeh Ziabari, S.M. Rozati. Carrier transport and bandgap shift in n-type degenerate ZnO thin films: The effect of bandedge nonparabolicity. *Physica B*, 407 (2012) 4512–4517.
- [70] H. Huang, Y. Ou, S. Xu, G. Fang, M. Li, X.Z. Zhao, *Appl Surf Sci.*, 254(2008) 2013–16.
- [71] R. Vinodkumar, I. Navas, S.R. Chalana, K.G. Gopchandran, V. Ganesan, Reji Philip, S.K. Sudheer, V.P. Mahadevan Pillai, *Applied Surface Science* 257 (2010) 708–716.
- [72] TingtinRen, Holly R. Baker, Kristin. M. poduska, *Thin Solid Films*, 515 (2007) 7976-7983.
- [73] V. Gokulakrishnan et al, *phys. Status Solidi A* 209, No. 8 (2012) 1481-1486 DOI 10.1002/pssa.201127619.

- [74] R. Vinodkumar, K.J.Lethy, D.Beena, A.P.Detty, I.Navas, U.V.Nayar, V.P.MahadevanPillai, V. Ganesan, V.R.Reddy, *Solar Energy Materials & Solar Cells* 94 (2010) 68–74.
- [75] Ruijin Hong, Hongji Qi, Jianbing Huang, Hongbo He, Zhengxiu Fan, Jianda Shao, *Thin Solid Films* 473 (2005) 58– 62.
- [76] M. Cich, K. Kim and S.T. Hwang, *Appl. Phys. Lett.* 73 (1998) 2116.
- [77] M.K. Patra, M. Manoth, V.K. Singh, G. SiddaramanaGowd, V.S. Choudhry, S.R. Vadera, N. Kumar *Journal of Luminescence* 129 (2009) 320–324.
- [78] F. H. Letter, H. R. Alves, A. Hofstaetter, D. M. Hofmann, B. K. Meyer, *Phys. Status Solidi (B)* 226 (2001) R4-R5.
- [79] T. Koida, S. F. Chichibu, A. Uedono, A. Tsukazaki, M. Kawasaki, T. Sota, Y. Segawa, H. Koinuma, *Appl. Phys. Lett.* Vol.82 No.4 (2003)532-534. DOI: 10.1063/1.1540220.
- [80] A. van Dijken, E. A. Meulenkaamp, D. Vanmaekelbergh, and A. Meijerink, *J. Lumin.* 87–89, (2000) 454-456.
- [81] OindrilaMondal ,Mrinal Pal, *J. Mater. Chem.*, 21 (2011) 18354–18358.
- [82] K. Vanheusden, C.H. Seager, W.L.Warren, D.R. Tallant, J.A. Voigt, *Appl. Phys. Lett.* 68 (1996) 403.
- [83] K. Vanheusden, C.H. Seager, W.L. Warren, D.R. Tallant, J. Caruso, M.J. Hampden-Smithb, T.T. Kodas, *Journal of Luminescence* 75 (1997) 11-16.
- [84] B. Lin, Z. Fu, Y. Jia, *Appl. Phys. Lett.* 79 (2001) 943.
- [85] V. A. L. Roy, A. B. Djurišić, W. K. Chan, J. Gao, H. F. Lui and C. Surya, *Appl. Phys. Lett.*, Vol. 83, No. 1, (2003) 141-143.DOI: 10.1063/1.1589184.
- [86] D. Li, Y.H. Leung, A.B. Djurišić, Z.T. Liu, M.H. Xie, S.L. Shi, S.J. Xu, W.K. Chan, *Appl. Phys. Lett.* 85 (2004) 1601-1603. DOI: 10.1063/1.1786375.
- [87] Y.M. Sun, Ph.D. Thesis, University of Science and Technology of China, July 2000.
- [88] X.Q. Wei, B.Y. Man, M. Liu, C.S. Xue, H.Z. Zhuang, C. Yang, *Physica B* 388 (2007) 145–152.
- [89] AparnaThankappan, Sheenu Thomas, and V. P. N. Nampoore, *Journal of Applied Physics* 112 (2012) 123104, DOI: 10.1063/1.4768930.
- [90] Cao H, Wu J Y, Ong H C, Dai J Y and Chang R P H , *Appl. Phys. Lett.*73 (1998) 572.
- [91] B. Karthikeyan, C.S. SuchandSandeep, T. Pandiyarajan, P. Venkatesan, R. Philip, *Applied Physics Letters* 95 (2009) 023118.
- [92] R. Vinodkumar, K.J. Lethy, P.R. Arunkumar, Renju R. Krishnan, N. VenugopalanPillai, V.P. MahadevanPillai, Reji Philip, *Materials Chemistry and Physics* 121 (2010) 406–413.
- [93] M. Sheik Bahae, A. A. Said, T. M. Wei, D. J. Hagan, and E. W. Vanstryland, *IEEE J. Quantum Electron.* 26, 760 (1990).
- [94] Lahtinen, J. A. *Phys. Rev. B* 1986, 33, 2550.

- [95] K.K. Nagaraja, S Pramodini, P Poorneshand H S Nagaraja, J. Phys. D: Appl. Phys. 46 (2013) 055106 (12pp), DOI:10.1088/0022-3727/46/5/055106
- [96] LittyIrimpan, V. P. N. Nampoore, and P. Radhakrishnan, journal of applied physics 103, 094914 (2008)
- [97] Kurian, P. A.; Vijayan, C.; Sandeep, C. S. S.; Philip, R.; Sathiyamoorthy, K. Nanotechnology 2007, 18, 075708.
- [98] Asunskis, D. J.; Bolotin, I. L.; Haley, J. E.; Urbas, A.; Hanley, L. J. Phys. Chem. C 2009, 113, 19824–19829.
- [99] Karthikeyan, B, Reji Philip. Appl. Phys. Lett. 2006, 88, 053104.
- [100] Karthikeyan, Anija, Reji Philip Appl. Phys. Lett.**88**, 053104 (2006).
- [101] K.K. Nagaraja, S. Pramodini, A. Santhosh Kumar, H.S. Nagaraja, P. Poornesh, DhananjayaKekuda, Optical Materials 35 (2013) 431–439.
- [102] H. Sekhar, D. NarayanaRao, J Nanopart Res (2012) 14:976, DOI 10.1007/s11051-012-0976-4.